Relationships among air-water interfacial area, capillary pressure, and water saturation for a sandy porous medium

Mark L. Brusseau,[1,2] Sheng Peng,[1,3] Gregory Schnaar,[1] and Molly S. Costanza-Robinson[4]

Received 23 February 2005; revised 18 November 2005; accepted 2 December 2005; published 14 March 2006.

[1] The relationships among air-water interfacial area, capillary pressure, and water saturation were investigated for a sandy, natural porous medium. Air-water interfacial areas as a function of water saturation were measured using two methods, gas phase partitioning tracer tests and synchrotron X-ray microtomography. The tracer test method provides a measure of effective total (capillary and film) interfacial area, whereas microtomography can be used to determine both capillary-associated and total areas (the latter is the focus of this study). Air-water interfacial areas determined with both methods increased continuously with decreasing water saturation. The areas measured with the tracer test method were significantly larger than those obtained from microtomography. The maximum values measured with the tracer test method approached the N_2/BET-measured specific solid surface area, whereas the maximum values measured by microtomography approached the smooth-sphere-calculated specific solid surface area. The interfacial area-saturation data were combined with capillary pressure-saturation data obtained from water drainage experiments to examine the relationship between total air-water interfacial area and capillary pressure. Air-water interfacial area was observed to increase monotonically with increasing capillary pressure and then to plateau at values that correspond to areas associated with residual water saturation. These results are consistent with previously reported theoretically and computationally based analyses of functional relationships between total nonwetting-wetting interfacial area and capillary pressure.

Citation: Brusseau, M. L., S. Peng, G. Schnaar, and M. S. Costanza-Robinson (2006), Relationships among air-water interfacial area, capillary pressure, and water saturation for a sandy porous medium, *Water Resour. Res.*, *42*, W03501, doi:10.1029/2005WR004058.

1. Introduction

[2] The air-water interface is critically important, given its influence on fluid flow, contaminant transport, and mass and energy transfer in unsaturated porous media. Potential relationships among air-water interfacial area, capillary pressure, and water saturation are of interest for example in modeling water flow in the vadose zone. Such relationships have been investigated in prior theoretical and modeling based research [e.g., *Leverett*, 1941; *Morrow*, 1970; *Gvirtzman and Roberts*, 1991; *Hassanizadeh and Gray*, 1993; *Cary*, 1994; *Reeves and Celia*, 1996; *Bradford and Leij*, 1997; *Or and Tuller*, 1999; *Berkowitz and Hansen*, 2001; *Held and Celia*, 2001; *Oostrom et al.*, 2001; *Dalla et al.*, 2002].

[3] Examination of air-water interfacial phenomena and the potential impact of system properties and conditions has been constrained by a lack of means by which to measure air-water interfacial areas. Recent advances in tracer [e.g., *Karkare and Fort*, 1996; *Brusseau et al.*, 1997; *Kim et al.*, 1997, 1999; *Anwar et al.*, 2000; *Schaefer et al.*, 2000; *Costanza-Robinson and Brusseau*, 2002] and imaging [e.g., *Montemagno and Gray*, 1995; *Wildenschild et al.*, 2002; *Culligan et al.*, 2004; *Al-Raoush and Willson*, 2005; *Schnaar and Brusseau*, 2005, 2006] methods have relaxed this constraint. The objective of this study was to evaluate the relationships among air-water interfacial area, capillary pressure and water saturation for a natural porous medium.

2. Materials and Methods

[4] Vinton soil (sandy, mixed thermic Typic Torrifluvent), collected locally in Tucson, Arizona, was used as the porous medium. It was sieved to remove the >2 mm fraction prior to use. The relevant properties of this medium are presented in Table 1. It is considered to be strongly water wetting. Soil water drainage experiments were conducted using the hanging water column and pressure chamber methods to obtain capillary pressure (h_c)−water saturation data [*Costanza-Robinson*, 2001]. The results of the water drainage experiment are presented in Figure 1. The *van Genuchten* [1980] function is observed to provide a reasonable fit to the data (with $\alpha = 0.026$, $m = 0.727$, and $n = 3.663$).

[5] The gas phase interfacial partitioning tracer test [*Brusseau et al.*, 1997; *Kim et al.*, 1999; *Costanza-Robinson and Brusseau*, 2002] was one method used to measure air-water interfacial areas. The tracer-based A_{ia}-S_w data used herein are taken from *Peng and Brusseau* [2005], from which more detailed information about these measurements can be obtained. Decane was used as the air-water interfacial

[1]Soil, Water and Environmental Science Department, University of Arizona, Tucson, Arizona, USA.
[2]Hydrology and Water Resources Department, University of Arizona, Tucson, Arizona, USA.
[3]Now at Geosystems Analysis, Tucson, Arizona, USA.
[4]Program of Environmental Studies and Department of Chemistry and Biochemistry, Middlebury College, Middlebury, Vermont, USA.

0043-1397/06/2005WR004058

Table 1. Relevant Properties of Vinton Soil

Parameter	Value
Mean diameter, mm	0.234
Uniformity coefficient U[a]	2.4
Specific surface area,[b] m^2/g	3.54
Porosity	0.39
Bulk density, g/cm^3	1.63
S_a,[c] cm^{-1}	156

[a] $U = d_{60}/d_{10}$, where d_{60} and d_{10} are the diameters for which 60 and 10% of the sample are finer by weight, respectively.

[b] Measured with the N_2/BET method by Quantachrome Instruments (Boynton Beach, Florida) and Micromeritics Corporation (Norcross, Georgia).

[c] Volume-normalized specific solid surface area calculated using the smooth sphere assumption: $S_a = 6(1 - n)/d$, where n is porosity and d is mean grain diameter.

partitioning tracer and methane as the nonreactive tracer. The column was made of stainless steel, and was 25 cm long by 2.2-cm diameter. Uniform water saturations (S_w) were obtained for the packed column by thoroughly mixing a predetermined amount of water with the porous medium, and packing the wetted material into the column. Tracer traveltimes were obtained by moment analysis of the breakthrough curves. Retardation factors for decane were calculated as the quotient of the decane and methane mean traveltimes. The specific air-water interfacial area (A_{ia}, L^{-1}), which represents interfacial area normalized by the porous medium volume, was obtained with knowledge of the retardation factor, interfacial partition coefficient, and porosity. The gas phase tracer method is considered to provide a measure of effective total air-water interfacial area, including both capillary-associated and film-associated areas [*Costanza-Robinson and Brusseau*, 2002].

[6] Synchrotron X-ray microtomography, a powerful method by which to characterize fluid distributions in porous media at the pore scale [e.g., *Wildenschild et al.*, 2002; *Culligan et al.*, 2004; *Al-Raoush and Willson*, 2005; *Schnaar and Brusseau*, 2005, 2006], was used as another method to determine A_{ia}. The microtomographic imaging was conducted at the GeoSoilEnviroCARS (GSECARS) BM-13D beam line at the Advanced Photon Source, Argonne National Laboratory, IL. Methods for collecting three-dimensional images of geologic and environmental samples using synchrotron X-ray microtomography, specific to the instrumentation at GSECARS, have been previously presented [e.g., *Sutton et al.*, 2002; *Wildenschild et al.*, 2002; *Culligan et al.*, 2004; *Schnaar and Brusseau*, 2005, 2006] and are not repeated herein.

[7] The porous medium was packed into thin-walled, X-ray-transparent acrylic columns (length = 3 cm, inner diameter = 0.5 cm). The bulk densities and porosities of the packed columns were very similar to those obtained for the larger packed columns used for the gas phase tracer tests. For the higher water saturations ($S_w > 0.8$), the columns were dry-packed, saturated with water, and then drained to the target S_w. For the lower saturations ($S_w < 0.5$), water was mixed with the porous medium prior to packing, identically to the method used for the gas phase partitioning tracer tests. The aqueous phase for all columns was doped with sodium iodide (13%) to enhance image contrast. The imaged sections were 6.2-mm long (of which the central 5.2 mm was used), and were obtained from the center of the columns. The spatial resolution was approximately 12 μm.

[8] The raw images were preprocessed and reconstructed with algorithms developed at GSECARS (http://cars9.uchicago.edu/software/index.html). The software package Blob3D, which was specifically developed for high-resolution X-ray microtomography applications [*Ketcham*, 2005], was used for additional image data processing and extraction of quantitative information. The total surface area of air, the nonwetting phase, was used to determine total air-water interfacial area. This is based on the assumption that all porous medium grains are solvated by water, thin films of which are not resolved by the microtomography method. Capillary-associated interfacial area was calculated as one half of the difference between the combined sum of the water phase and air phase surface areas and the solid phase surface area [e.g., *Dalla et al.*, 2002].

[9] The A_{ia}-h_c relationships were developed by combining two independently measured data sets, A_{ia}-S_w data measured using the gas phase partitioning tracer method or microtomography, and h_c-S_w data obtained with the water drainage measurements. For the microtomography data, measured A_{ia} values were matched through the associated S_w values to corresponding h_c values obtained from the characteristic curve. This approach was possible for only three points for the gas phase tracer data because the majority of the A_{ia} measurements were obtained at water saturations below the range spanned by the characteristic curve. Thus A_{ia} values were also calculated for a given set of S_w values using a regression equation calibrated to the measured A_{ia}-S_w data. Values of h_c were calculated for the same set of S_w values using the best fit h_c-S_w function. These two data sets were combined to yield the A_{ia}-h_c data. This approach was also used for the microtomography data.

3. Results and Discussion

[10] The A_{is}-S_w data obtained from the gas phase tracer tests reported by *Peng and Brusseau* [2005] are presented in Figure 2. Specific air-water interfacial area is observed to increase with decreasing water saturation. The largest mea-

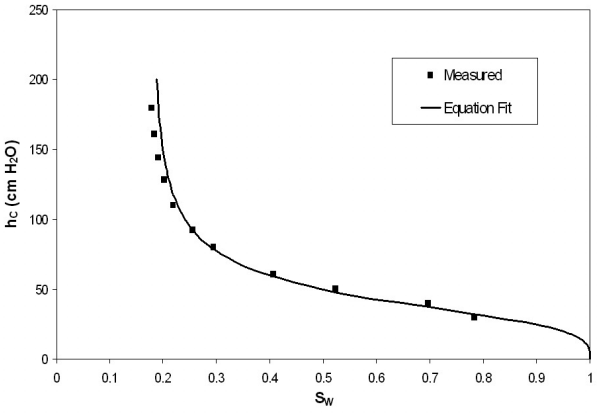

Figure 1. Measured and fitted capillary pressure (h_c)–water saturation (S_w) characteristic curve for Vinton soil. The equation fit was produced using the van Genuchten function [*van Genuchten*, 1980].

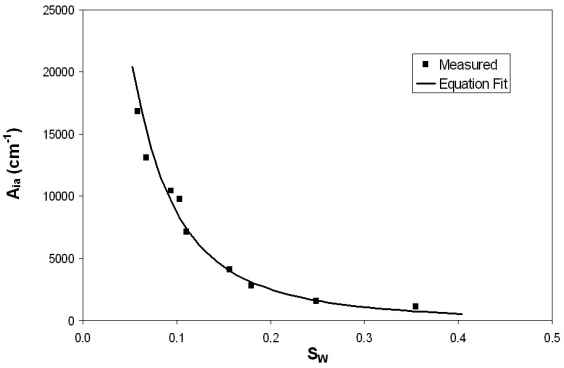

Figure 2. Total specific air-water interfacial area (A_{ia}) as a function of water saturation (S_w) determined from the gas phase partitioning tracer test method. An empirical equation of similar form as the van Genuchten equation was calibrated to the measured data [*Peng and Brusseau*, 2005]: $A_{ia} = s[1 + (\alpha S_w)^a]^{-b} - c$, where s is the specific solid surface area and α, b, and c are calibration coefficients (with $\alpha = 19.78$, b = 1.35, c = 104, and a = 1/(2 − b)).

sured value is approximately one third the volume-normalized specific solid surface area (~51700 cm^{-1}) determined from N_2/BET measurement. These results are consistent with those of prior studies using the gas phase partitioning tracer method [*Kim et al.*, 1999; *Costanza-Robinson and Brusseau*, 2002].

[11] The A_{ia}-S_w data obtained from the synchrotron X-ray microtomography are presented in Figure 3. Total A_{ia} is observed to increase linearly with decreasing S_w over the measured range. This behavior is consistent with that observed in theoretical and computational studies of the relationship between total nonwetting-wetting interfacial area and S_w [e.g., *Leverett*, 1941; *Or and Tuller*, 1999; *Oostrom et al.*, 2001; *Dalla et al.*, 2002]. Conversely, capillary-associated A_{ia} appears to first increase and then decrease with decreasing S_w. This is consistent with the results of prior theoretical, computational, and experimental studies [e.g., *Morrow*, 1970; *Gvirtzman and Roberts*, 1991; *Hassanizadeh and Gray*, 1993; *Reeves and Celia*, 1996; *Berkowitz and Hansen*, 2001; *Held and Celia*, 2001; *Dalla et al.*, 2002; *Cheng et al.*, 2004; *Culligan et al.*, 2004]. The magnitudes of the measured total and capillary-associated A_{ia} values are similar to the respective computationally based A_{ia} values reported by *Dalla et al.* [2002].

[12] As described above, total A_{ia} was obtained for the microtomography data by measuring the total specific surface area of air, given their equivalency when all solid surfaces are solvated by water. An extrapolated total specific surface area of 155 cm^{-1} is obtained for $S_w = 0$ using the regression equation reported in Figure 3. This value is very similar to the volume-normalized specific solid surface area (156 cm^{-1}) calculated using the smooth sphere assumption. This similarity supports the consistency of the microtomography measurements, given that solid phase and air phase surface areas are equivalent at $S_w = 0$. Similar regressions are obtained with and without inclusion of the lower-saturation data, for which the columns were packed with prewetted porous media. This suggests that the method of water introduction does not appear to affect the measured total A_{ia} values for this system. It may, however, be of more significance for the individual capillary and film components of total A_{ia}.

[13] The A_{ia} values measured with the gas phase tracer method are significantly larger than those measured by microtomography. As noted above, as S_w approaches zero, the A_{ia} values measured with the tracer test method approach the N_2/BET-measured specific solid surface area. In contrast, the A_{ia} values measured by microtomography approach a maximum value that is very similar to the smooth-sphere-based specific solid surface area. The specific solid surface area measured with the N_2/BET method incorporates the contributions of microscopic surface heterogeneity (e.g., surface roughness, microporosity). It is hypothesized that the gas phase tracer method provides some measure of the air-water interface associated with this microscopic surface heterogeneity, as well as other features for which the resolution of the microtomography method is insufficient to measure. Conversely, the specific solid surface area calculated using the smooth sphere assumption excludes contributions from features such as surface roughness and microporosity. Given that interfacial areas associ-

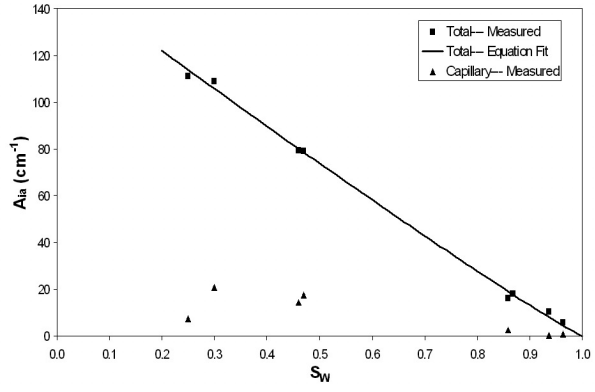

Figure 3. Total and capillary-associated specific air-water interfacial areas (A_{ia}) as a function of water saturation (S_w) determined from microtomography. The regression equation is $A_{ia} = 154.8(1 - S_w)^{1.07}$.

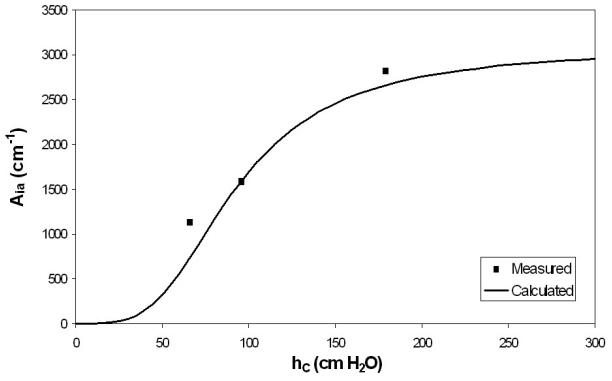

Figure 4. Measured and calculated total specific air-water interfacial area (A_{ia}) as a function of capillary pressure (h_c), determined by combining the gas phase partitioning tracer test A_{ia}-S_w data with the capillary pressure (h_c)-water saturation (S_w) data.

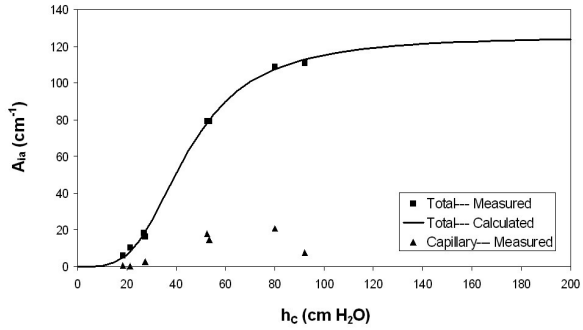

Figure 5. Total (measured and calculated) and capillary-associated (measured) specific air-water interfacial areas (A_{ia}) as a function of capillary pressure (h_c), determined by combining the microtomography A_{ia}-S_w data with the capillary pressure (h_c)–water saturation (S_w) data.

ated with these features are generally not resolved with microtomography, it would appear reasonable that the microtomography-based total interfacial areas approach the smooth-sphere-based specific solid surface area.

[14] The A_{ia}-h_c relationships obtained using the gas phase tracer and microtomography A_{ia} data are presented in Figures 4 and 5, respectively. Both data sets exhibit the same overall behavior, wherein total A_{ia} initially increases monotonically with increasing capillary pressure, and then plateaus at a value that corresponds to interfacial areas associated with residual water saturation. These results are consistent with previously reported theoretical and computational based analyses of functional relationships between total nonwetting-wetting interfacial area and capillary pressure [e.g., *Or and Tuller*, 1999; *Dalla et al.*, 2002]. In contrast, the capillary-associated interfacial area appears to first increase and then decrease with increasing capillary pressure (Figure 5). This behavior is consistent with the results of prior theoretical, computational, and experimental studies [e.g., *Gvirtzman and Roberts*, 1991; *Hassanizadeh and Gray*, 1993; *Reeves and Celia*, 1996; *Held and Celia*, 2001; *Dalla et al.*, 2002; *Cheng et al.*, 2004; *Culligan et al.*, 2004].

4. Summary

[15] The relationships among air-water interfacial area, capillary pressure, and water saturation were investigated for a sandy, natural porous medium. Air-water interfacial areas as a function of water saturation were measured using two methods, gas phase partitioning tracer tests and synchrotron X-ray microtomography. The areas determined with the tracer test method were significantly larger than those determined from microtomography. This difference may reflect the inability of the microtomography method to fully measure interfacial area associated with microscopic surface heterogeneities and other features. Thus the gas phase tracer method may be more suitable for characterizing ''total'' interfacial areas relevant to the transport and fate of contaminants whose retention and transformation is influenced by air-water interfacial phenomena. For analysis of fluid flow, it may be desirable to characterize air-water interfacial areas associated with specific domains, which is generally problematic with the tracer-based methods. The microtomography method appears particularly useful for characterizing capillary-associated interfacial area, which is especially relevant for bulk fluid flow.

[16] The interfacial area-saturation data were combined with capillary pressure-saturation data obtained from water drainage experiments to examine the relationship between air-water interfacial area and capillary pressure. The magnitude of the total air-water interfacial area was observed to increase with increasing capillary pressure to an asymptotic value dependant upon residual water content. These results are consistent with previously reported theoretical and computational based analyses of functional relationships between total interfacial area and capillary pressure.

[17] The relationship between total air-water interfacial area and capillary pressure was quantified empirically by coupling an equation describing the relationship between air-water interfacial area and water saturation with a capillary pressure-saturation function. Two such A_{ia}-S_w equations were reported herein, both of which provided excellent matches to the respective measured data. These equations were coupled with the van Genuchten h_c-S_w function to produce a continuous A_{ia}-h_c relationship. Such a function may be useful for example in applications involving modeling of fluid flow. The applicability of this approach will of course be limited by the constraints associated with the associated underlying functions.

[18] **Acknowledgments.** This research was funded by the USDA National Research Initiative Program, with additional support from the NIEHS Superfund Basic Research Program. The microtomography imaging was performed at GeoSoilEnviroCARS (Sector 13), Advanced Photon Source (APS), Argonne National Laboratory. GeoSoilEnviroCARS is supported by the National Science Foundation-Earth Sciences (EAR-0217473), Department of Energy-Geosciences (DE-FG01-94ER14466) and the State of Illinois. Use of the APS was supported by the U.S. Department of Energy, Basic Energy Sciences, Office of Energy Research, under contract W-31-109-Eng-38. We thank Asami Murao, Art Warrick, Shlomo Neuman, and the anonymous reviewers for their assistance.

References

Al-Raoush, R., and C. S. Willson (2005), A pore-scale investigation of a multiphase porous media system, *J. Contam. Hydrol.*, *77*, 67–89.

Anwar, A. H. M. F., M. Bettahar, and U. Matsubayashi (2000), A method for determining air-water interfacial area in variably saturated porous media, *J. Contam. Hydrol.*, *43*, 129–146.

Berkowitz, B., and D. P. Hansen (2001), A numerical study of the distribution of water in partially saturated porous rock, *Transp. Porous Media*, *45*, 303–319.

Bradford, S. A., and F. J. Leij (1997), Estimating interfacial areas for multi-fluid soil systems, *J. Contam. Hydrol.*, *27*, 83–105.

Brusseau, M. L., J. Popovicova, and J. A. K. Silva (1997), Characterizing gas-water interfacial and bulk-water partitioning for gas phase transport of organic contaminants in unsaturated porous media, *Environ. Sci. Technol.*, *31*, 1645–1649.

Cary, J. W. (1994), Estimating the surface area of fluid phase interfaces in porous media, *J. Contam. Hydrol.*, *15*, 243–248.

Cheng, J.-T., L. J. Pyrak-Nolte, D. D. Nolte, and N. J. Giordano (2004), Linking pressure and saturation through interfacial areas in porous media, *Geophys. Res. Lett.*, *31*, L08502, doi:10.1029/2003GL019282.

Costanza-Robinson, M. S. (2001), Elucidation of retention processes governing the transport of volatile organic compounds in unsaturated soil systems, Ph.D. thesis, Univ. of Ariz, Tucson.

Costanza-Robinson, M. S., and M. L. Brusseau (2002), Air-water interfacial areas in unsaturated soils: Evaluation of interfacial domains, *Water Resour. Res.*, *38*(10), 1195, doi:10.1029/2001WR000738.

Culligan, K. A., D. Wildenschild, B. S. B. Christensen, W. Gray, M. L. Rivers, and A. F. B. Tompson (2004), Interfacial area measurements for unsaturated flow through a porous medium, *Water Resour. Res.*, *40*, W12413, doi:10.1029/2004WR003278.

Dalla, E., M. Hilpert, and C. T. Miller (2002), Computation of the interfacial area for two-fluid porous medium systems, *J. Contam. Hydrol.*, *56*, 25–48.

Gvirtzman, H., and P. V. Roberts (1991), Pore scale spatial analysis of two immiscible fluids in porous media, *Water Resour. Res.*, *27*, 1165–1176.

Hassanizadeh, S. M., and W. G. Gray (1993), Thermodynamic basis of capillary pressure in porous media, *Water Resour. Res.*, *29*, 3389–3405.

Held, R. J., and M. A. Celia (2001), Modeling support of functional relationships between capillary pressure, saturation, interfacial area and common lines, *Adv. Water Resour.*, *24*, 325–343.

Karkare, M. V., and T. Fort (1996), Determination of the air-water interfacial area in wet "unsaturated" porous media, *Langmuir*, *12*, 2041–4044.

Ketcham, R. A. (2005), Computational methods for quantitative analysis of three-dimensional features in geological systems, *Geosphere*, *1*, 32–41.

Kim, H., P. S. C. Rao, and M. D. Annable (1997), Determination of effective air-water interfacial area in partially saturated porous media using surfactant adsorption, *Water Resour. Res.*, *33*, 2705–2711.

Kim, H., P. S. C. Rao, and M. D. Annable (1999), Gaseous tracer technique for estimating air-water interfacial areas and interface mobility, *Soil Sci. Soc. Am. J.*, *63*, 1554–1560.

Leverett, M. C. (1941), Capillary behavior in porous solids, *Trans. Am. Inst. Min. Metall. Eng.*, *142*, 152–169.

Montemagno, C. D., and W. G. Gray (1995), Photoluminescent volumetric imaging: A technique for the exploration of multi-phase flow and transport in porous media, *Geophys. Res. Lett.*, *22*, 425–428.

Morrow, N. R. (1970), Physics and thermodynamics of capillary action in porous media, *Ind. Eng. Chem.*, *62*, 32–56.

Oostrom, M., M. D. White, and M. L. Brusseau (2001), Theoretical estimation of free and entrapped nonwetting-wetting fluid interfacial areas in porous media, *Adv. Water Resour.*, *24*, 887–898.

Or, D., and M. Tuller (1999), Liquid retention and interfacial area in variably saturated porous media: Upscaling from single-pore to sample-scale model, *Water Resour. Res.*, *35*, 3591–3605.

Peng, S., and M. L. Brusseau (2005), The impact of soil texture on air-water interfacial areas in unsaturated sandy porous media, *Water Resour. Res.*, *41*, W03021, doi:10.1029/2004WR003233.

Reeves, P. C., and M. A. Celia (1996), A functional relationship between capillary pressure, saturation, and interfacial area as revealed by a pore-scale network model, *Water Resour. Res.*, *32*, 2345–2358.

Schaefer, C. E., D. A. Dicarlo, and M. J. Blunt (2000), Experimental measurement of air-water interfacial area during gravity drainage and secondary imbibition in porous media, *Water Resour. Res.*, *36*, 885–890.

Schnaar, G., and M. L. Brusseau (2005), Pore-scale characterization of organic immiscible-liquid morphology in natural porous media using synchrotron X-ray microtomography, *Environ. Sci. Technol.*, *39*, 8403–8410.

Schnaar, G., and M. L. Brusseau (2006), Characterizing pore-scale configuration of organic immiscible liquid in multi-phase systems with synchrotron X-ray microtomography, *Vadose Zone J.*, in press.

Sutton, S. R., P. M. Bertsch, M. Newville, M. L. Rivers, A. Lanzirotti, and P. Eng (2002), Microfluroescence and microtomography analyses of heterogeneous Earth and environmental materials, in *Applications of Synchrotron Radiation in Low-Temperature Geochemistry and Environmental Sciences*, edited by P. A. Fenter et al., pp. 429–483, Mineral. Soc. of Am., Chantilly, Va.

van Genuchten, M. T. (1980), A closed-form equation for predicting the hydraulic conductivity of unsaturated soils, *Soil Sci. Soc. Am. J.*, *44*, 892–898.

Wildenschild, D., J. W. Hopmans, C. M. P. Vaz, M. L. Rivers, and D. Rikard (2002), Using X-ray computed tomography in hydrology: Systems, resolutions, and limitations, *J. Hydrol.*, *267*, 285–297.

M. L. Brusseau and G. Schnaar, Soil, Water and Environmental Science Department, 429 Shantz Building, 38, University of Arizona, Tucson, AZ 85721, USA. (brusseau@ag.arizona.edu)

M. S. Costanza-Robinson, Department of Chemistry and Biochemistry, 466 Bicentennial Hall, Middlebury College, Middlebury, VT 05753, USA.

S. Peng, Geosystems Analysis, 2015 North Forbes Boulevard, Suite 105, Tucson, AZ 85745-1458, USA.